Atmospheric Pressure Chemical Vapour Deposition of Fluorine-doped Tin(IV) Oxide from Fluoroalkyltin Precursors

J. E. Stanley, A. C. Swain, K. C. Molloy, D. W. H. Rankin, H. E. Robertson and B. F. Johnston.
Appl. Organomet. Chem., 2005, 644-657.

DOI: 10.1002/aoc.721

Atmospheric Pressure Chemical Vapour Deposition of F-Doped Tin(IV) Oxide from Fluoroalkyltin Precursors

Joanne E Stanley, Anthony C Swain and Kieran C Molloy *

Department of Chemistry, University of Bath, Bath BA2 7AY, UK

David W H Rankin, Heather E Robertson and Blair F Johnston

School of Chemistry, University of Edinburgh, West Mains Road, Edinburgh, EH9 3JJ, UK

Perfluoroalkytin compounds $R_{(4-n)}Sn(R_f)_n$ (R = Me, Et, Bu, $R_f = C_4F_9$, n = 1; R = Bu, $R_f = C_4F_9$, n = 2, 3; R = Bu, $R_f = C_6F_{13}$, n = 1) have been synthesised, characterised by ^{1}H, ^{13}C, ^{19}F and ^{119}Sn NMR and evaluated a precursors for the atmospheric pressure CVD (APCVD) of F-doped SnO_2 thin films. All precursors were sufficiently volatile at in the range 84 – 136°C and glass substrate temperatures of *ca*. 550°C to yield high quality films with *ca.* 0.79 – 2.02% fluorine incorporation, save for $Bu_3SnC_6F_{13}$ which incorporated < 0.05% fluorine. Films were characterised by XRD, SEM, thickness, haze, emissivity, sheet resistance. The fastest growth rates and highest quality films were obtained from $Et_3SnC_4F_9$. An electron diffraction study of $Me_3SnC_4F_9$ revealed four conformations of which only the two of lowest abundance showed close F···Sn contacts which could plausibly be associated with halogen transfer to tin and in each case it was fluorine attached to either the γ- or δ-carbon atoms of the R_f chain.

KEYWORDS: fluoroalkyltin, F-doped tin oxide, CVD, thin film

* Address for correspondence; e-mail: k.c.molloy@bath.ac.uk

Graphical Abstract

Fluoroalkyltin compounds have been used as CVD precursors for the deposition of thin films of F-doped SnO_2.

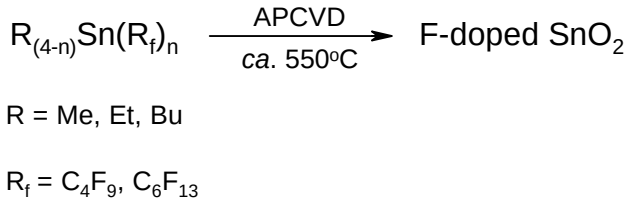

INTRODUCTION

Doped tin oxide films are arguably the most studied of the transparent conducting oxide thin films, as they have found widespread applications in various optoelectronic devices including electrochromic displays, liquid crystal displays and solar cells.[1-9] Of all the dopants employed (P,[10,11] , As [12] Sb[13,14] etc), fluorine is the most common as it generates films of high conductivity and optical clarity.[15-17] Thin films of SnO_2, including F-doped materials, can be achieved by a number of routes (sol-gel,[18-23] rf sputtering,[24,25] spray pyrolysis [26-30]) though chemical vapour deposition (CVD) is the method of choice for large-scale coatings. This is particularly pertinent in the coating of architectural glass, where F:SnO_2 has been widely exploited as a solar control device to reduce energy loss from buildings and in which the doped tin oxide film acts by being transparent to visible wavelengths but reflective in the infrared.[31-33]

Conventional CVD experiments have employed both a volatile tin source [e.g. $SnMe_4$,[34-36] $SnCl_4$, [37-40] $SnCl_2$,[41] $Sn(NMe_2)_4$ [42]] in conjunction with both oxygen (e.g. O_2,[36] H_2O [43]) and fluorine precursors (e.g. F_2,[44] NH_4F,[45] HF,[46,16] $BrCF_3$,[15] various CFCs,[10] CF_3CO_2H [29,47]). In comparison, relatively few attempts have been made to deposit F-doped SnO_2 from a *single-source precursor*, though the advantages of eliminating toxic and/or environmentally unfriendly precursors from the CVD process are clear. Molecules which incorporate a direct Sn-F bond often lack sufficient volatility for CVD experiments by virtue of their tendency to incorporate Sn-F:→Sn bridges (e.g. R_3SnF),[48,49] but species such as (β-diketonate)$_2$Sn(F)(OR) are now available and have been successfully employed in sol-gel approaches to F:SnO_2.[22,23,50]

To retain volatility, most attempts to develop single-source precursors for F:SnO_2 have incorporated the dopant element into a more complex ligand system rather than having it directly bonded to tin, and successful CVD of F:SnO_2 has been achieved from $Sn[OCH(CF_3)_2]_4.2HNMe_2$,[51] $Sn[OCH(CF_3)_2]_2.L$ (L = $HNMe_2$, C_5H_5N),[52,51] $Sn(O_2CCF_3)_2$ [53] and $Bu_2Sn(O_2CCF_3)_2$.[54] To our knowledge, there is only one instance of the use of perfluoroalkytin species as precursors [$(C_4H_9C{\equiv}C)_3SnCH_2CH_2CF_3$, $(C_4H_9C{\equiv}C)_3SnC_6H_4F$-*o*][55,56] which have generated F:SnO_2 in sol-gel procedures by a γ-F transfer mechanism. Fully fluorinated alkyl

chains may be anticipated to deliver the halogen to the tin from any of the available carbon centres, with a β-F transfer mechanism possibly the most likely:[57]

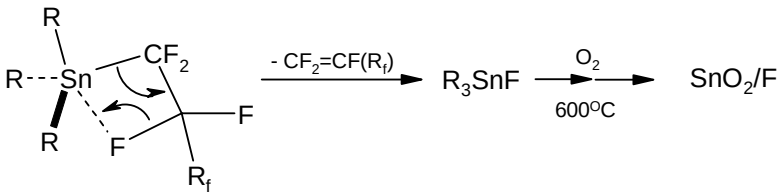

However, the possibility of alternative decomposition pathways e.g involving radicals, cannot be excluded.

Fluoroorganotins have been known for many years, though they have proved less synthetically amenable than non-fluorinated organotins. The majority of known compounds contain only one fluorinated group (R_3SnR_f),[58,59,57,60] with relatively few examples of compounds containing additional R_f groups,[61,62] particularly the homoleptic $Sn(R_f)_4$.[63] Of the known synthetic protocols (Table 1), reaction of hexaorganoditins with R_fI yields product mixtures which are often difficult to separate,[59,58,57] while fluoro-organomagnesium reagents are themselves relatively difficult to prepare.[61] The latter can be more conveniently prepared indirectly, by reaction of RMgX with R_fI,[63] and this has enabled the Grignard route to afford a number of $(C_3F_7)_nSnR_{4-n}$ species in variable yields.[63] Similar methodology has proved less effective in the case of organolithium reagents,[60] though it has been used as a route to fluorovinyltin compounds.[64,65] Less widespread methodologies have involved organocadmium reagents [66] and oxidative addition of R_fI to divalent tin species.[67]

In this paper we report the synthesis of a range of $R_nSn(R_f)_{4-n}$ and their use as atmospheric pressure chemical vapour deposition (APCVD) precursors for the deposition of F:SnO_2 thin films. Included in this report is the gas-phase structure of $Me_3(C_4F_9)Sn$, determined using a combination of electron diffraction and computational methods.

EXPERIMENTAL

General

Infrared spectra (cm^{-1}) were recorded as liquid films between NaCl plates using a Nicolet 510P FT-IR spectrophotometer, and elemental analyses were performed using an Carlo-Erba Strumentazione E.A. model 1106 microanalyser operating at 500°C. ^1H and ^{13}C NMR spectra

were recorded on a Jeol JNM-GX270 FT spectrometer while ^{19}F and ^{119}Sn NMR spectra were recorded on a Jeol JNM-EX400 FT machine, all using saturated $CDCl_3$ solutions unless indicated otherwise; chemical shifts are in ppm with respect to either Me_4Si, Me_4Sn or $CFCl_3$, coupling constants in Hz. Details of our Mössbauer spectrometer and related procedures are given elsewhere; [68] data are in mm s^{-1}. Dry solvents were obtained by distillation under inert atmosphere from the following drying agents: sodium-benzophenone (toluene, ether, THF), calcium hydride (CH_2Cl_2), sodium (hexane). Standard Schlenk techniques were used throughout. Starting materials were commercially obtained and used without further purification.

Syntheses

Tributyl(perfluorobutyl)tin - $Bu_3SnC_4F_9$ (**1**). Isopropyl chloride (3.48 g, 44 mmol) in dry ether (30 ml) was added slowly to magnesium turnings (1.20 g, 50 mmol) to prepare the Grignard reagent isopropylmagnesium chloride. This was transferred by canula into a pressure equalising dropping funnel then added dropwise to freshly distilled perfluorobutyl iodide (15.32 g, 44 mmol) in dry ether (100 ml) at -78°C. The solution was stirred at this temperature for one hour to allow exchange to take place. Tributyltin chloride (9.72 g, 30 mmol) was then added slowly by syringe, the solution warmed to -40°C and stirred at this temperature for two hours. The flask was then allowed to warm slowly to room temperature overnight with stirring, and the solvent removed *in vacuo* to yield an oil and a white solid. The mixture was extracted into 40°-60° petroleum ether and the solid removed by filtration. The solvent was removed *in vacuo* to leave a colourless oil, which by ^{119}Sn NMR was found to be a mixture of tributylperfluorobutyltin and unreacted tributyltin chloride. The mixture was separated by column chromatography using silica gel as the stationary phase and 40°-60° petroleum ether as the eluant. Tributyl(perfluorobutyl)tin was eluted as the first fraction and removal of the solvent *in vacuo* yielded the product as a colourless oil (8.33 g, 55%). Analysis : Found (calc. for $C_{16}H_{27}F_9Sn$) : C 37.8 (37.7)%; H 5.37 (5.36)%. ^1H NMR : 0.92 [9H, t, $CH_3(CH_2)_3$], $^3J(^1H\text{-}^1H)$ 7 Hz; 1.22 [6H, m, C_4H_9]; 1.35 [6H, m, C_4H_9]; 1.60 [6H, m, C_4H_9].^{13}C NMR: 10.5 [$CH_3(CH_2)_3$]; 13.5 [$CH_3(CH_2)_2CH_2$] [$^1J(^{13}C\text{-}^{119}Sn)$ 333 Hz]; 27.1 [$CH_3CH_2(CH_2)_2$]; 28.3 [$CH_3CH_2CH_2CH_2$]. C-F carbons not observed.^{19}F NMR : -126.6 [m, $CF_3CF_2(CF_2)_2$]; -

119.2 [m, $CF_3CF_2CF_2CF_2$]; -118.2 [m, $CF_3(CF_2)_2CF_2$]; -81.7 [m, $CF_3(CF_2)_3$]. ^{119}Sn NMR: -1.6, t, $^2J(^{119}Sn\text{-}^{19}F)$ 190 Hz. Mössbauer data: IS = 1.39; QS = 1.58. IR: 2961, 2928, 2859, 1466, 1420, 1379, 1346, 1235, 1154, 1084, 1007, 961, 793, 743.

Bis-(perfluorobutyl)dibutyltin - $Bu_2Sn(C_4F_9)_2$ (**2**). The method described previously for (**1**) was utilised with isopropyl chloride (54.98 g, 63 mmol) added to magnesium turnings (1.60 g, 66 mmol) in dry ether (30 ml). The Grignard reagent was added dropwise to freshly distilled perfluorobutyl iodide (22.68 g, 66 mmol) at -78°C. Dibutyltin dichloride (6.40 g, 21 mmol) dissolved in dry ether (5 ml) was added slowly by syringe at -78°C, then the flask warmed to -40°C and stirred at this temperature for two hours. Following the previously described work-up procedure, dibutyl-bis-(perfluorobutyl)tin was obtained as a colourless liquid (4.58 g, 32%). Analysis : Found (calc. for $C_{16}H_{18}F_{18}Sn$) : C 29.6 (28.6)%; H 2.74 (2.71)%. ^{1}H NMR: 0.94 [6H, t, $CH_3(CH_2)_3$], $^3J(^1H\text{-}^1H)$ 7 Hz; 1.37 [4H, m, C_4H_9]; 1.60 [8H, m, C_4H_9]. ^{13}C NMR: 13.3 [$CH_3(CH_2)_3$]; 13.6 [$CH_3(CH_2)_2CH_2$] [$^1J(^{13}C\text{-}^{119}Sn)$ 358 Hz]; 26.9 [$CH_3CH_2(CH_2)_2$]; 27.4 [$CH_3CH_2CH_2CH_2$]. C-F carbons not observed. ^{19}F NMR: -126.7 [m, $CF_3CF_2(CF_2)_2$]; -118.4 [m, $CF_3CF_2CF_2CF_2$]; -113.9 [m, $CF_3(CF_2)_2CF_2$]; -81.8 [m, $CF_3(CF_2)_3$]. ^{119}Sn NMR: -56.0, quin, $^2J(^{119}Sn\text{-}^{19}F)$ 237 Hz. Mössbauer data : IS = 1.46; QS = 1.75. IR: 2965, 2932, 2865, 1468, 1348, 1238, 1132, 1071, 1009, 795, 745, 681, 644.

Tris-(perfluorobutyl)butyltin - $BuSn(C_4F_9)_3$ (**3**). The methodology described for (**1**) was repeated with isopropyl chloride (6.44 g, 82 mmol) reacted with magnesium turnings (2.00 g, 82 mmol). The resultant Grignard reagent was added dropwise to freshly distilled perfluorobutyl iodide (29.19 g, 82 mmol) at -78°C. Butyltin trichloride (5.10 g, 18 mmol) was added slowly by syringe then the mixture warmed to -40°C and stirred at this temperature for two hours. Following the work-up procedure described for (**1**), (**3**) was obtained as a colourless liquid (2.74 g, 18%). Analysis : Found (calc. for $C_{16}H_9F_{27}Sn$) : C 24.5 (23.1)%; H 1.51 (1.09)%. ^{1}H NMR: 0.96 [3H, t, $CH_3(CH_2)_3$], $^3J(^1H\text{-}^1H)$ 7Hz; 1.42 [2H, m, C_4H_9]; 1.60 [4H, m, C_4H_9]. ^{13}C NMR : 13.0 [$CH_3(CH_2)_3$]; 13.2 [$CH_3(CH_2)_2CH_2$] [$^1J(^{13}C\text{-}^{119}Sn)$ 395 Hz]; 26.6 [$CH_3CH_2(CH_2)_2$]; 26.9 [$CH_3CH_2CH_2CH_2$]. C-F carbons not observed. ^{19}F NMR: -126.8 [m, $CF_3CF_2(CF_2)_2$]; -117.8 [m, $CF_3CF_2CF_2CF_2$]; -108.6 [m, $CF_3(CF_2)_2CF_2$]; -81.9 [m, $CF_3(CF_2)_3$].

^{119}Sn NMR: -154.5, sept, ^{2}J(^{119}Sn-^{19}F) 300 Hz. Mössbauer data: IS = 1.44; QS =1.49. IR: 2969, 2882, 1470, 1348, 1237, 1134, 1101, 997, 851, 777, 745, 683, 534.

Tributyl(perfluorohexyl)tin - $Bu_3SnC_6F_{13}$ (**4**). The methodology described for (**1**) was employed with isopropyl chloride (1.89 g, 24 mmol) and magnesium turnings (0.60 g, 25 mmol). The resultant Grignard reagent was added to freshly distilled perfluorohexyl iodide (10.93 g, 25 mmol) at -78°C and stirred at this temperature for one hour. Tributyltin chloride (5.30 g, 16 mmol) was added slowly by syringe then the flask was warmed to -40°C and stirred for a further two hours. Following the work-up procedure described for (**1**), (**4**) was isolated as a colourless liquid (1.70 g, 17%). Analysis : Found (calc. for $C_{18}H_{27}F_{13}Sn$) : C 35.5 (35.5)%; H 4.45 (4.48)%.^{1}H NMR: 0.92 [9H, t, C*H*$_3$(CH$_2$)$_3$], ^{3}J(^{1}H-^{1}H) 7 Hz; 1.21 [6H, m, C$_4$H$_9$]; 1.35 [6H, m, C$_4$H$_9$]; 1.57 [6H, m, C$_4$H$_9$]. ^{13}C NMR: 10.6 [*C*H$_3$(CH$_2$)$_3$]; 13.5 [CH$_3$(CH$_2$)$_2$*C*H$_2$] [^{1}J(^{13}C-^{119}Sn) 329 Hz]; 27.1 [CH$_3$*C*H$_2$(CH$_2$)$_2$]; 28.3 [CH$_3$CH$_2$*C*H$_2$CH$_2$]. C-F carbons not observed. ^{19}F NMR: -126.7 [m, CF$_3$C*F*$_2$(CF$_2$)$_4$]; -123.5 [m, CF$_3$CF$_2$C*F*$_2$(CF$_2$)$_3$]; -122.5 [m, CF$_3$(CF$_2$)$_2$C*F*$_2$(CF$_2$)$_2$]; -118.3 [m, CF$_3$(CF$_2$)$_3$C*F*$_2$CF$_2$]; -117.9 [m, CF$_3$(CF$_2$)$_4$C*F*$_2$]; -81.4 [m, C*F*$_3$(CF$_2$)$_5$]. ^{119}Sn NMR: -0.6, t, ^{2}J(^{119}Sn-^{19}F) 191 Hz. Mössbauer data: IS = 1.35; QS = 1.57. IR: 2961, 2926, 2857, 1659. 1466, 1360, 1238, 1206, 1144, 1115, 1084, 1017, 882, 735, 652.

Triethyl(perfluorobutyl)tin - $Et_3SnC_4F_9$ (**5**). The methodology described for (**1**) was followed using isopropyl chloride (2.80 g, 36 mmol) and magnesium turnings (0.90 g, 37 mmol). The resultant Grignard reagent was added to freshly distilled perfluorobutyl iodide (12.18 g, 35 mmol) at -78°C, then triethyltin chloride (5.70 g, 24 mmol) added after stirring for one hour. The flask was warmed to -40°C and stirred for a further two hours at this temperature. The work-up procedure described for (**1**) yielded (**5**) as a colourless liquid (3.68 g, 37%). Analysis : Found (calc. for $C_{10}H_{15}F_9Sn$) : C 28.4 (28.3)%; H 3.56 (3.57)%. ^{1}H NMR: 1.19 [9H, t, C*H*$_3$CH$_2$], ^{3}J(^{1}H-^{1}H) 7 Hz; 1.27 [6H, q, CH$_3$C*H*$_2$]. ^{13}C NMR: 10.1 [*C*H$_3$CH$_2$]; 10.3 [CH$_3$*C*H$_2$] [^{1}J(^{13}C-^{119}Sn) = 331 Hz]. C-F carbons not observed. ^{19}F NMR: -126.7 [m, CF$_3$C*F*$_2$(CF$_2$)$_2$]; -119.5 [m, CF$_3$CF$_2$C*F*$_2$CF$_2$]; -117.9 [m, CF$_3$(CF$_2$)$_2$C*F*$_2$]; -81.8 [m, C*F*$_3$(CF$_2$)$_3$]. ^{119}Sn NMR: 3.6, t, ^{2}J(^{119}Sn-^{19}F) 190 Hz. Mössbauer data: IS = 1.36; QS = 1.65. IR: 2957, 2878, 1470, 1383, 1348, 1237, 1154, 1084, 1047, 1006, 961, 743, 679, 519.

Trimethyl(perfluorobutyl)tin - $Me_3SnC_4F_9$ (**6**) was prepared by the same methodology as (**1**); yield 42%. ^{1}H NMR: 0.43 [9H, s, CH_3], $^{2}J(^{1}H\text{-}^{119}Sn)$ 58.6 Hz. ^{13}C NMR: -8.86 [CH_3], $^{1}J(^{13}C\text{-}^{119,117}Sn)$ = 362, 346 Hz, 109.4 (q, CF_3) $^{1}J(^{19}F\text{-}^{13}C)$ = 74 Hz, 112.4 (t, CF_2) $^{1}J(^{19}F\text{-}^{13}C)$ = 61 Hz, 116.2 (t, CF_2) $^{1}J(^{19}F\text{-}^{13}C)$ = 67 Hz, 119.1 (t, CF_2) $^{1}J(^{19}F\text{-}^{13}C)$ = 67 Hz. ^{19}F NMR: -126.5 [t, $CF_3CF_2C\mathit{F}_2CF_2$] $^{3}J(^{19}F\text{-}^{19}F)$ = 22 Hz; -121.2 [t, $CF_3(CF_2)_2C\mathit{F}_2$] $^{3}J(^{19}F\text{-}^{19}F)$ = 23 Hz, $^{2}J(^{119}Sn\text{-}^{19}F)$ = 225 Hz; -120.2 [t, $CF_3C\mathit{F}_2(CF_2)_2$] $^{3}J(^{19}F\text{-}^{19}F)$ = 19 Hz; -81.7 [tt, $C\mathit{F}_3(CF_2)_3$] $^{3}J(^{19}F\text{-}^{19}F)$ = 19 Hz, $^{4}J(^{19}F\text{-}^{19}F)$ = 7 Hz. ^{119}Sn NMR: 25.3, t, $^{2}J(^{119}Sn\text{-}^{19}F)$ 225 Hz.

Chemical Vapour Deposition

Details of our apparatus are given elsewhere.[69] The entire system consists of a horizontal cold wall reactor with associated gas lines and electrical heater controls. The precursor was heated in a stainless steel bubbler which was encased in an oven in which the temperature of the precursor could be measured accurately by a thermocouple positioned inside the bubbler. The pipework inside the oven contained a by-pass system which enabled the gas flows and temperatures to be set before the nitrogen carrier gas flow was turned to the bubbler to transport the vaporised precursor. Following the turning of the valves to direct the gas flow to the bubbler, the precursor was swept from the bubbler and then mixed with nitrogen diluent and oxygen before being transported from the oven. The mixture was then transported along the heated external pipework to the CVD reactor. Before the vapour reached the CVD reactor, it was passed through a baffle to promote laminar flow. After passing through the baffle, the precursor vapour was passed directly into the reactor chamber which is 8 mm high, 40 mm wide and 300 mm long contained within ceiling tiles and walls of silica plates.

The glass substrate is positioned upon a large graphite susceptor which is heated by three Watlow-fire rod cartridge heaters; the temperature of the graphite block is maintained by a Watlow series 965 controller which monitors the temperature by means of thermocouples positioned inside the block. The graphite susceptor was held inside a large silica tube (330 mm long, 100 mm diameter) suspended between stainless steel flanges upon which many of the electrical and gas line fittings are fixed. Air-tight seals are provided by “Viton” O-rings.

All of the glass substrates were cleaned in an identical manner prior to use by washing thoroughly in sequence with tap water, copious amounts of distilled water and finally a generous amount of isopropyl alcohol (IPA), then allowed to drain. The glass was always prepared immediately prior to a deposition experiment to ensure as clean a substrate surface as possible.

The bubbler temperatures required to generate sufficient volatility for each precursor were 136 (**1**), 121 (**2**), 109 (**3**), 131 (**4**) and 84^{o}C (**5**). As all precursors were liquids, excessive temperatures for the heater tapes were not necessary as there were no problems with condensation of precursors within the pipework. Therefore, a consistent temperature of 200°C was found to be satisfactory for the transport of all precursors between bubbler and reactor. Suitable gas flows were also found to be fairly universal for all compounds tested and those initially optimised for precursor **1** (diluent N_2: 1.0 Lmin$^{-1;}$ carrier N_2: 1.0 Lmin^{-1}; O_2: 0.6 Lmin^{-1}) were found to be adequate for the other materials. Substrate temperatures were either 564^{o}C (**1** - **4**) or 546^{o}C (**5**) and the duration of the deposition processes were 15 (**1**), 7 (**2**), 10 (**3**), 25 (**4**) and 1 minute (**5**).

Film Analysis

The X-ray diffraction equipment consisted of a Philips PW1130 generator operating at 45 kV and 40 mA to power a copper long fine focus X-ray tube. A PW 1820 goniometer fitted with glancing-angle optics and proportional X-ray detector was used. The non-focusing thin film optics employed a ¼ degree primary beam slit to irradiate the specimen at a fixed incident angle of 1.5°. Diffraction radiation from the sample was collimated with a flat plate collimator and passed through a graphite flat crystal monochromator to isolate diffracted copper Kα peaks onto the detector. The equipment was situated in a total enclosure to provide radiation safety for the highly collimated narrow beams of X-rays. Data were acquired by a PW1710 microprocessor and processed using Philips APD VMS software. Crystalline phases were identified from the International Centre for Diffraction Data (ICDD) database. Samples of coating for XRD were of approximate dimensions 1.5 $\times$ 2.0 cm. Crystallite size was determined from line broadening using the Scherrer equation.[70] The instrumental effect was removed using the NIST SRM660 lanthanum hexaboride standard. These operating

conditions were used in preference to conventional Bragg-Brentano optics for thin films to give an order of magnitude increase in count rate from a fixed volume of coating with little contribution from the substrate.

Film thickness was determined by etching a thin strip of the film with zinc powder and 50% HCl solution. This created a step in the film which was measured with a Dektak stylus technique.

Haze was measured on a Pacific Scientific Hazeguard meter and with a barium fluoride detector. The calculation of haze was carried out by measurement of the specular light and diffusive light. Specular light is defined as light transmitted straight through the sample within ± 2.5° of normal incidence and the diffusive light is defined as light scattered beyond 2.5°. The initial measurement was carried out with the specular detector slot closed and therefore a value for the sum of the specular light and the diffusive light is obtained. The specular light slot is then opened and a measurement of the diffusive light is obtained.

$$\% \text{ Haze} = [\text{Diffusive Light} / (\text{Diffusive} + \text{Specular Light})] \times 100$$

Emissivity data were then calculated from the infra-red reflectance spectra, measured using a two-beam Perkin Elmer 883 machine and measured against a rhodium mirror standard, using the formula:[71]

$$Emissivity = 1 - \frac{\int_{5\mu}^{50\mu} R_\lambda P_\lambda d\lambda}{\int_{5\mu}^{50\mu} P_\lambda d\lambda}$$

i.e. integral of total emittance between 5 and 50 μm divided by the integral from 5 - 50 μm of the total emittance of a blackbody at room temperature.

Sheet resistance was measured with a four point probe on an electrically isolated scribed circle of film (□ = 25 cm^2) and corrected using a conversion factor, the value being dependent

on the diameter of the scribed circle. Knowing the sheet resistance and the film thickness, the resistivity was determined by:

$$\text{Resistivity } (\Omega \text{ cm}) = \text{Sheet resistance } (\Omega/\square) \times \text{Thickness (cm)}$$

XRF measurements were made on a Philips PW1400 machine fitted with a scandium target X-ray tube. The penetration depth achieved was between 9 and 10 microns, so the result obtained was throughout the thickness of the coating. The analysis was performed on approximately 6 cm^2 of material.

Theoretical methods

Calculations were performed on a DEC Alpha APX 1000A workstation using the GAUSSIAN 94 program.[72] An extensive search of the potential energy surface of $Me_3SnC_4F_9$ (**6**) was undertaken at the HF/3-21G* level in order to locate all structurally stable conformers. In total four conformers were found, all with C_1 symmetry (Figure 1). Further geometry optimisations were then undertaken for all minima with the D95 basis set [73] (a full double zeta basis set) including a double zeta set on tin [74] (15s, 11p, 7d/ 11s, 7p, 4d) at the HF level. The subsequent two sets of calculations used the LanL2DZ [75-77] effective core potential (ECP) basis set (incorporating relativistic effects) for tin and D95 for the remaining atoms at the HF and MP2 levels of theory. Vibrational frequencies were calculated from analytic second derivatives up the D95 (F, C, H, O), LanL2DZ (Sn)/HF level to confirm all conformers as local minima on the potential energy surface. The force constants obtained from these calculations were subsequently used to construct harmonic force fields for all conformers using the ASYM40 program.[78,79] As no fully assigned vibrational spectra are available for **6** to scale the force fields, a scaling factor of 0.9 was adopted for bond stretches, angle bends and torsions.[80] The scaled harmonic force fields were then used to provide estimates of amplitudes of vibration (u) for use in the gas-phase electron diffraction (GED) refinements. The results of the highest level of these theoretical calculations [MP2/LanL2DZ (Sn) – D95] can be seen in Table 2; a complete tabulation of the results at all levels is available as ESI.

Gas-phase electron diffraction

Data were collected on Kodak Electron Image plates using the Edinburgh gas diffraction apparatus.[81] An accelerating voltage of *ca.* 40 kV (electron wavelength *ca.* 6.0 pm) was used, with sample and nozzle temperatures of ~400 K and ~450 K respectively; nozzle-to-plate distances were 95.57 and 252.33 mm. The weighting points for the off-diagonal weight matrices, correlation parameters and scale factors for the two camera distances are given in Table 3, together with electron wavelengths. The wavelengths were determined from the scattering patterns of benzene vapour, recorded immediately after the patterns of $Me_3SnC_4F_9$ and analysed in exactly the same way, to minimise systematic errors in wavelengths and camera distances. A PDS densitometer at the Institute of Astronomy in Cambridge was used to convert the intensity patterns into digital form. Data reduction and least-squares refinements were carried out using the new 'ed@ed' program,[82] employing the scattering factors of Ross *et al*.[83]

Based on the *ab initio* MO calculations, a theoretical model was written for $Me_3SnC_4F_9$, allowing for the co-existence of three conformers, each with C_1 symmetry. The three lowest energy conformers found in the *ab initio* study [Figures 1(a), (b) and (c)] were included in the model. The fourth conformer, which was 16.6 kJ mol^{-1} higher in energy relative to the lowest energy conformer, was ignored, as it would only have made up a tiny percentage of the conformer mixture at the experimental temperature. Twenty-eight parameters were required in order to model the compound in the desired symmetry. These consisted of eight bonded-distance parameters (four average bond lengths and four difference parameters), eighteen angle parameters and two parameters that controlled the relative amounts of conformers. In the description of the parameters given below, the term average applies to the average for all conformers modelled. The distance parameters are the average C-H (p_1), the average Sn-C (p_2), the difference between the average of Sn(1)-C(6), Sn(1)-C(7) and Sn(1)-C(8) and the longer Sn(1)-C(2) (p_3), the average C-C (p_4), the average C-F (p_5), the difference between the average of C(2)-F(9/10) and the average of the other C-F bonds (p_6), the difference between the average of C(3)-F(11/12) and the average of the C(4)-F(13/14) and C(5)-F(15/16/17) bonds (p_7) and the difference between the average of C(4)-F(13/14) and the average C(5)-F(15/16/17) (p_8). The angle parameters are the average C(4)-C(5)-$F_{(terminal)}$

angle (assuming local C_3 symmetry on the terminal CF_3 group) (p_9), the average F-C-F angle for the three CF_2 groups (p_{10}), C(3)-C(4)-C(5) (in conformer 2) (p_{11}), C(2)-C(3)-C(4) (in conformer 2) (p_{12}), Sn(1)-C(2)-C(3) (in conformer 2) (p_{13}), C(2)-Sn(1)-C(6) (p_{14}), C(7)-Sn(1)-C(8) (p_{15}), the average of C(7&8)-Sn(1)-C(6) (assuming local C_s symmetry of the $SnMe_3$ group, with C(2)-Sn(1)-C(6) lying on the mirror plane) (p_{16}) and the average Sn-C-H angle (p_{17}). Parameters 18, 19 and 20 have the same definitions as parameters 11, 12 and 13 but apply to conformer 1. Parameters 21, 22 and 23 also have the same definitions as parameters 11, 12 and 13 but apply to conformer 3. Parameter 24 is a torsion angle used for the approximately anti-configured C-C- C-C torsion angles in all three conformers. These include C(3)-C(2)-Sn(1)-C(6), Sn(1)-C(2)-C(3)-C(4) and C(2)-C(3)-C(4)-C(5) in conformer 1, C(3)-C(2)-Sn(1)-C(6) and Sn(1)-C(2)-C(3)-C(4) in conformer 2 and C(3)-C(2)-Sn(1)-C(6) and C(2)-C(3)-C(4)-C(5) in conformer 3. While individual torsion angles could have been used as unique independent parameters, it was felt that the calculated values were sufficiently similar to warrant grouping them together in this way. Fixed difference values were assigned to parameter 24, with values of -3.0° for C(2)-C(3)-C(4)-C(5) in conformer 1 (p_{24}-3.0°) and 6.0° for C(2)-C(3)-C(4)-C(5) in conformer 3 (p_{24}+6.0°). A parameter, p_{25}, was also needed to model the approximately *gauche* C-C-C-C torsion angles, C(2)-C(3)-C(4)-C(5) in conformer 2 and Sn(1)-C(2)-C(3)-C(4) in conformer 3. The torsion angle C(3)-C(4)-C(5)-F(15), which controls the rotation of the terminal CF_3 group in all conformers, is p_{26}. The final two parameters, p_{27} and p_{28}, control the fractional amounts of conformers 2 and 1 respectively, with the weight of conformer 3 automatically being calculated as 1.0 - (p_{27} + p_{28}). The refined and calculated parameters can be found in Table 4.

The starting parameters for the r_a refinements were taken from the theoretical geometry optimised at the MP2 level. The theoretical Cartesian force fields was obtained and converted into a force field described by a set of symmetry coordinates using a version of the ASYM40 program modified to work for molecules with more than 40 atoms. All 28 geometric parameters and 26 groups of vibrational amplitudes were refined, using 24 flexible restraints on geometric parameters (Table 4) and 25 restraints on amplitudes of vibration (*see* ESI) according to the SARACEN method.[84,85]

RESULTS AND DISCUSSION

Synthesis and Spectroscopy

A series of perfluoroalkytin compounds $R_{(4-n)}Sn(R_f)_n$ (**1** - **6**) has been prepared employing the methodology of Seyferth *et al*.:[63]

$$Mg + {}^{i}PrCl \xrightarrow[r.\,t.]{Et_2O} {}^{i}PrMgCl \xrightarrow[-78^{O}C]{R_fI\,/\,Et_2O} R_fMgCl + {}^{i}PrI$$

$$nR_fMgCl + R_{(4-n)}SnCl_n \xrightarrow[-40^{O}C]{Et_2O} R_{(4-n)}Sn(R_f)_n + nMgCl_2$$

R = Bu, $R_f = C_4F_9$, n = 1 (**1**), n = 2 (**2**), n = 3 (**3**)

R = Bu, $R_f = C_6F_{13}$, n = 1 (**4**)

R = Et, $R_f = C_4F_9$, n = 1 (**5**)

R = Me, $R_f = C_4F_9$, n = 1 (**6**)

The synthesis of $Bu_3SnC_4F_9$ (**1**) illustrates the importance of choice of synthetic protocol in realising viable yields of the fluoroalkyltin compounds. Direct synthesis of the Grignard C_4F_9MgI from magnesium and C_4F_9I followed by addition of Bu_3SnCl yielded a crude product mixture (^{119}Sn NMR) consisting of unreacted organotin (155.9 ppm) in addition to a quantity of Bu_3SnI (86.2 ppm) and $Bu_3SnC_4F_9$ (-1.6 ppm). Vacuum distillation of the mix was unsuccessful in yielding a clean product due to the similarity in boiling points of all the tributyltin compounds. Separation by column chromatography required a very long column (≈ 30 cm) as the triorganotins eluted only slightly more slowly from the column than the desired tetraorganotin. The perfluoroalkyltin compound was ultimately isolated in a very poor yield (10%).

Similarly, the organolithium reagent C_4F_9Li, prepared *in situ* from MeLi and C_4F_9I, required an extremely low temperature (-100°C) to prevent decomposition resulting in poor conversion to the desired product (**1**) (11% after column chromatography, as above). These findings are consistent with a previous report on this reaction.[60]

The most effective and reproducible method for the synthesis of the fluoroalkyltins involved the indirect formation of the Grignard, R_fMgI, from iPrMgCl and C_4F_9I. While this reaction was also found to be extremely temperature sensitive and care had to be taken to ensure the

temperature remained at -78°C during this step, adequate formation of the perfluoromagnesium iodide could be realised over a minimum of 1 h. Reagent quantities were chosen to form 50% excess equivalents of the required Grignard reagent (based on 100% conversion) for reaction with the organotin chloride to allow for decomposition and incomplete conversion. This was especially important for the synthesis of compounds in which more than one chloride was to be replaced, to reduce the complexity of the final product mixture. The reaction of the fluorinated Grignard reagent with the organotin chloride proceeded better at a slightly elevated temperature (-40°C), and to achieve a reasonable yield this temperature had to be maintained for at least 2 h. The yield of **1** by this method was increased to 55%.

It was generally found that the yields decreased as more fluorinated groups were introduced, and overall were in the range 18 – 55%. All compounds are air stable, colourless liquids.

NMR spectra confirm the composition of the compounds. The magnitudes of the $^{1}J(Sn\text{-}C_H)$ for **1** - **6** (331 – 395 Hz) are in the appropriate region for four-coordinate organotin species (300 - 400 Hz).[86,87] There is an increase in $^{1}J(Sn\text{-}C_H)$ in as the number of R_f groups incorporated increases (**1**: 333; **2**: 358; **3**: 395 Hz), due to the high electronegativity of the R_f ligands, which have a stronger demand for 5*p*(Sn) character in the Sn-C_F bond as the R groups are progressively replaced by R_f ligands; the *s*-character of the Sn-C_H bonds increases accordingly.

^{119}Sn NMR proved the best measure of compound purity and validation of the number of R_f groups introduced. All the compounds showed strong coupling of tin to the fluorine atoms of the α-carbon, but there were no couplings with more distant fluorines displayed. The 2n + 1 multiplicity (observation of the triplet, quintet or septet) of the tin signal proved diagnostic of the presence of 2, 4 and 6 α-fluorines, respectively. The upfield shift of $\delta(^{119}Sn)$ in the series **1** - **3** (-1.6, -56.0, -154.5 ppm, respectively) is consistent with other reports e.g. $Me_2Sn(C_3F_7)_2$, -22.8; $MeSn(C_3F_7)_3$, -131 ppm.[63] $^{2}J(^{119}Sn\text{-}^{19}F)$ increases as more R_f groups are introduced (e.g. **1**: 190; **2**: 237; **3**: 300 Hz), which is also consistent with earlier reports e.g. $MeSn(C_3F_7)_3$, 308; $Sn(C_3F_7)_4$, 387 Hz.[63]

The electronegativity imbalance between R and R_f is also manifest in observable Mössbauer quadrupole splittings for **1** – **5** (1.49 – 1.75 mms^{-1}). The q. s. for Me_3SnCF_3 has been reported as 1.38 mm s^{-1}.[88]

Structural Study

The computational study of $Me_3SnC_4F_9$ (**6**) showed that there are four stable conformers (Figure 1,a – d), two of which are likely to be significantly populated at the temperature of the electron diffraction experiments (*ca.* 400 K). This is supported by the analysis of the GED data, which shows that the only conformers in which a fluorine atom gets close enough to tin for exchange to occur easily (conformers 3 and 4) must only exist in small quantities (*ca.* 2% for conformer 3, < 1% for conformer 4). However, the experimental data indicate that even a large fraction of conformer 3, in which the C_4F_9 chain is less twisted than in the computed high-energy conformer 4, has a negative effect on the refinement.

The optimum fit of the GED data was found for a mixture of 65% conformer 2, 33% conformer 1 and 2% conformer 3, while calculations predict that the mixture is 86% conformer 2 and 13% conformer 1 (1% conformer 3). These values were obtained by manual adjustment of the two weight parameters, p_{27} and p_{28}.

The geometrical parameters obtained in the refinement are listed in Table 4; interatomic distances and amplitudes of vibration, and lists of the most significant elements of the least squares correlation matrix are available as ESI. The final R factors were R_G = 0.027 and R_D = 0.039. Figures showing the experimental and final difference molecular scattering intensity curves and the radial distribution curves are available as ESI. Elucidation of the GED structure of $Me_3SnC_4F_9$ was made particularly tricky by the poor quality of the data recorded at the short camera distance, although the experiment was repeated several times. This is reflected in the large number of restraints that were employed in the refinement. Without these restraints even parameters such as Sn-C and C-F, which would normally be expected to refine well, were not particularly well behaved and were found to refine to unrealistic values. It is unlikely that a successful refinement could have been carried out in this instance without the results from the *ab initio* calculations. Comparing the Sn-C bond lengths from the GED experiment with those calculated *ab initio* at the MP2 level of theory, it was found that

the average was 0.7 pm shorter in the GED refinement (214.7 pm GED, 215.4 pm MP2). The calculations that did not use the LanL2 pseudo-potential on tin predicted the average Sn-C bond length to be 217.9 pm. Inclusion of the pseudo-potential results in a shortening of the Sn-C distance by 2.1 pm at the HF level and 2.3 pm at the MP2 level. The GED value suggests that using a pseudo-potential on tin is important in order to obtain accurate theoretical structures.

Calculations also found the Sn(1)-C(2) bond of the fluoroalkyltin moiety to be longer than the other Sn-C bonds by around 9 pm, reflecting the presence of the fluorine substituents on the butyl chain. This is consistent with the trend in $^{1}J(^{119}Sn\text{-}^{13}C_{H})$ couplings, which indicate a concentration of 5*p*(Sn) character in the Sn-C_F bonds, hence the relative lengthening of the latter. A 9.0(5) pm difference was also found in the GED study, although this value was restrained quite closely to that calculated at the MP2 level. C-C bond lengths varied very little on changing the level of the theoretical calculations. A decrease of around 0.9 pm (from 154.2 pm to 153.3 pm) was observed on going from the HF/D95 to the MP2 level. There was reasonable agreement between these values and the value of 155.0(3) pm from the GED refinement. The average C-F bond length was found to vary more than the C-C distances. At the MP2 level the average C-F distance was found to be 136.1 pm, around 3 pm longer than in both the HF/D95 and HF/LanL2DZ(Sn)-D95(F,C,H) calculations. This is likely to be a result of better treatment of the lone pairs on the fluorine atoms with the inclusion of electron correlation at the MP2 level. The GED value of 135.9(1) pm for the average C-F bond length is in excellent agreement with that obtained in the MP2 calculations. Similarity between the values calculated at the MP2 and HF/3-21G* levels (both 136.1 pm) is fortuitous, a consequence of cancellation of errors in the HF/3-21G* calculations.

Bond angles generally varied little in the series of *ab initio* calculations. However, there was a substantial difference in the angle Sn(1)-C(2)-C(3) for the three major conformers, being calculated as 115.3° for both conformer 1 and conformer 2, but as much as 121.7° for conformer 3. Despite the fairly large differences between conformers, <Sn(1)-C(2)-C(3) did not change much with different theoretical treatments, decreasing by 1.3 to 1.5° from the HF/D95 level to the MP2 level in each case. C(2)-C(3)-C(4) also varied with conformation, but the extent of this variation changed little with the level of calculation. The GED values for

these angles in the three conformers are in good agreement with theory, although once again restraints were necessary to obtain stability in the refinement. C(3)-C(4)-C(5) varied little with the level of calculations, and differences between conformers were smaller, with values of 114.5° in conformer 1, 117.2° in conformer 2 and 115.4° in conformer 3 at the MP2 level. The bond angles with Sn at the apex [C(2)-Sn(1)-C(6), C(7)-Sn(1)-C(8), C(2)-Sn(1)-C(7) and C(2)-Sn(1)-C(8)] did not show the same sensitivity to the inclusion of the pseudo-potential on tin as the Sn-C bond lengths, and angles changed by less than 1° as the level of calculation was varied. The average F-C-F angle for the CF_2 groups also changed little, even on going to the MP2 level of theory, despite the C-F bond lengths being significantly longer at this level.

The unrestrained *anti* twist parameter, p_{24}, which controlled the torsion angle C(2)-C(3)-C(4)-C(5) in conformers 1 and 3, was found to agree well with the value calculated *ab initio*, the GED refinement giving 164.6(17)°, compared with the calculated (MP2) values of 161.6° in conformer 1 and 168.4° in conformer 3. The *gauche* twist parameter, p_{25}, which controls the torsion angles C(2)-C(3)-C(4)-C(5) in conformer 2 and Sn(1)-C(2)-C(3)-C(4) in conformer 3, was, however, found to be substantially smaller in the GED refinement.

Of significance to the CVD study is the relative disposition of tin and a suitable fluorine atom, such that transfer of the halogen to the metal can readily occur, thereby affording a doped SnO_2 film. In all of the four conformers the fluorines of the α-CF_2 group are within 3 Å of tin, but are oriented away from the metal. In addition, the three low-energy conformers (Fig. 1 a – c) have close Sn···F contacts with the fluorine atoms attached to the β-carbon, with Sn…F(11) distances between 320 and 330 pm, although in none of these cases does the halogen approach the tin *trans* to a CH_3 group, a scenario which would be most effective in transferring the halogen to the tin *via* a five-coordinated transition state. Furthermore, there is no apparent lengthening of the C-F bond associated with the short Sn····F contact. In contrast, conformers 3 and 4 offer more realistic pathways for fluorine transfer to tin. The high-energy, low-abundance conformer 4 has a close contact with the fluorine atom of the δ-carbon [Sn···F(17); 322 pm] in which such a five-coordinated arrangement, albeit somewhat distorted [<F(17)···Sn-C(8): 163.2^o] is observed. In conformer 3, the closest F…Sn contact is 327.4 pm, with an F(14)…Sn-C(6) angle of 165.3°. In both conformer 3 and conformer 4 the C-F that is thus linked to the tin atom is calculated to be 1.2 pm longer than its neighbouring C-F bond(s).

Film Deposition

Compounds **1** - **5** have been screened as potential CVD precursors for F:SnO_2, using an atmospheric pressure CVD reactor described elsewhere.[69] In all cases, the substrate used was 4 mm glass which had been undercoated with a thin film of SiCO to act as a blocking layer to prevent sodium diffusion into the deposited film. The reactor temperatures (*ca*. 550 ^oC) were found to produce good transparent films which adhered well to the glass substrate and could not be removed without relatively harsh treatment. Lower temperatures resulted in a vast decrease in the growth rates, while powdery deposits were obtained at higher temperatures. No attempt has been made in this study to optimise deposition parameters.

It was found that precursor (bubbler) temperatures generally in excess of 100^oC were required for reasonable growth rates, suggesting that the precursors are not remarkably volatile. The butyltin derivatives **1** - **4** were found to require much higher temperatures (109 – 136 ^oC) than the ethyltin compound **5** (84 ^oC), which suggests a higher degree of volatility for precursors containing smaller R groups. Also, it was observed that the acceptable bubbler temperature decreased through the series **1** - **3** (136, 121, 109 ^oC, respectively) as the number of fluorinated groups increased, showing a greater volatility with additional fluorine incorporation. Consequently, deposition times required to produce films of thickness adequate for characterisation (*ca*. 3000 Å) varied for $R_{4-n}Sn(R_f)_n$ in the order Bu > Et and n = 1 > 2 ≈ 3 (see Experimental). Films grown from the butyltin compounds **1** – **4** were found to favour deposition at the front end of the substrate directly after the precursor inlet and only coated the first 5 - 6 cm of the glass, while the film grown from the ethyltin derivative **5** had a much more uniform appearance and spanned the total length of the glass. Therefore, for commercial production where a high growth rate and consistent film uniformity is required, small R groups appear to be preferential. $Et_3SnC_4F_9$ (**5**), which required a bubbler temperature of 84 ^oC and deposited *ca*. 3000 Å thick films of F:SnO_2 in 1 minute at 546^oC, was the most effective of the precursors evaluated in this study.

Film Characterisation

Glancing Angle X-Ray diffraction confirmed the film composition as crystalline SnO_2 in all cases; a representative diffraction pattern is shown in Figure 2 for the film grown from **1**. From line broadening measurements of the (110) reflection it was possible to estimate the approximate crystallite sizes of the samples, which lie in the range 119 – 264 Å (**3**, **4** respectively **n**). All the films showed similar preferred orientations when compared to a standard sample of SnO_2. The degree of orientation can be quantified as the ratio of the intensity of the (200) reflection to the total integrated intensity of the diffraction pattern, expressed as a percentage; for a random orientation of SnO_2 this ratio would be 7%. The degree of preferred (200) orientation is at a minimum for films grown from the tributyltin derivatives **1**, **4** (13.8, 9.5%), increasing as the number of R_f groups increases (**2**: 17.8; **3**: 19.2%) but maximising for the triethyltin precursor **5** (25.5%). Previous work has shown that SnO_2 films grown along the (200) direction contain less structural defects [40,10] and therefore give better performance for such applications as solar cells.[89]

Scanning Electron Microscopy (SEM) of the film deposited from **1** (Figure 3) shows a uniform morphology and a smooth film surface; the photograph clearly shows the SiCO undercoat on which the fluorine-doped tin oxide coating has subsequently been deposited.

For all films, thickness, haze, emissivity, sheet resistance, resistivity and fluorine content were measured (Table 5) and are compared with data typical of F:SnO_2 films used in solar control coatings.[90] Fluorine incorporation in the range 1- 8%,[91,15] optimising at *ca*. 3%,[92] has been found enhance the film properties, leading to low resistivity and low emissivity (the ability of a material to re-radiate absorbed energy into a colder environment; low-E coatings are desirable in cold climates to prevent heat loss); good visual appearance is indicated by a low haze, which increases as the film becomes more cloudy.

All precursors produced fluorine-doped tin oxide films establishing that the perfluoroalkyltin compounds were capable of acting as single-source precursors. Reasonable success was achieved in trying to obtain films of approximately 3000 Å thickness, the approximate dimension of commercial F:SnO_2 films, from precursors with which there were sufficient quantities to perform several runs. Due to the small synthetic quantities of precursors **3** and **4**, growth rate was not optimised and the best film derived from **3** was extremely thick (6165 Å),

while a very thin film (2000 Å) was obtained from precursor **4**. Data from these films can therefore only be taken as a guide to optimum film properties. As might be expected, low emissivity and resistivity were noted for the thick film grown from **3**, but at the expense of very high haze (4.10%). In contrast, higher emissivity and resistivity were found for the thin film grown from precursor **4**, although the haze was also reasonably high (0.50%) for a film of only 2000 Å thickness. Compound **4** does not seem a promising precursor for F:SnO_2. The properties of the film derived from precursor **3** are also not a significant improvement on the measurements given for a standard coating given its enhanced thickness. Due to the difficult and expensive synthesis of the precursors, and, more importantly, the production of better quality films from other precursors, it was decided not to synthesise additional material in order to perform further deposition experiments.

Films derived from **1**, **2** and **5** have properties which approach those of commercial films derived from a dual-source approach, which suggests that more detailed deposition study could lead to an even more competitive properties. From the trends in data available from this initial study, it appears that increasing the number of R_f groups in the precursor diminishes the resultant film quality (**1** *vs* **2**). Moreover, data from **3**, **4** also suggest that increased fluorine content in the precursor, either from more or longer R_f groups, also has a detrimental effect on film quality. The film derived from **5**, which has the best overall portfolio of properties and accrues at the highest growth rate, further implies one R_f group is sufficient and that $(C_2H_5)_nSn$ is favoured over $(C_4H_9)_nSn$, a feature that we have noted in other related precursor systems, e.g. $Et_3SnO_2CCF_3$ *vs* $Bu_3SnO_2CCF_3$.[93]

The fluorine content of the films shows no discernable pattern and raises a number of issues. From compounds (**1**) and (**2**), which contain an increasing number of fluorinated groups, it can be seen that the incorporation of additional fluorine into the precursor leads to an increase in the quantity of fluorine found in the resultant tin oxide film. Furthermore, the fluorine content determined for the film grown from precursor (**5**) is similar to that found for (**1**), which is reasonable given that the compounds have an identical $R_3SnC_4F_9$ formulation. However, a reduced fluorine content was observed from $BuSn(C_4F_9)_3$ (**3**) with three fluorinated ligands, the reason for which is unclear but could suggest an alternative or competing decomposition mechanism is operating. The extremely low fluorine content found

in the film deposited from $Bu_3SnC_6F_{13}$ (**4**) was unexpected, but probably explains the extremely poor set of properties exhibited by this film (Table 5).

The incorporation of fluorine from the precursor into the SnO_2 film is inevitably related to both the structure of the precursor and its decomposition mechanism. Previous works on the pyrolysis of fluoroorganotin compounds have established that (i) α-elimination is feasible where no other alternative is possible (decomposition of Me_3SnCF_3 to Me_3SnF and *cyclo*-C_3F_6 at 150^{o}C),[59] (ii) β-elimination is not as facile as might be expected ($Me_3SnC_2F_5$ remains 91% intact after 72 h at 200^{o}C; small amounts of C_2F_5H are detected) but is enhanced by the presence of branched-chain fluoroalkyl groups [$Me_3SnCF(CF_3)_2$ decomposes to Me_3SnF and $F_2C=C(F)CF_3$ at 150^{o}C over a 64 h period] [57] and (iii) γ-F competes well with β-H transfer [$R_3SnCH_2CH_2CF_3$ decomposes to yield similar amounts of R_3SnF / *cyclo*-$C_3H_4F_2$ and R_3SnH / $H_2C=C(H)CF_3$ at 200 – 300^{o}C over 2 h; R = $C{\equiv}CC_4H_9$].[55] Our structural study of $Me_3SnC_4F_9$ shows that approach of γ-F and δ-F to tin along reaction coordinates that favour formation of five-coordinated transition states occurs in conformers 3 and 4 respectively, with lengthening of the C-F bonds, and that transfer of fluorine from these sources are most likely. The experimental amount of conformer 3 is only 1%, but this value is very uncertain, and the calculated amount is 12% at 400 K (the temperature of GED experiment), rising to 21% at 830 K (the temperature of the CVD experiment). Conformer 4 is calculated to account for fewer than 1% of the molecules at 400 K but 3.6% at 830 K, so it too could be involved in the fluorine-transfer process. In addition, if either or both of the γ- and δ-F sites are responsible for the doping, the low fluorine content of the film produced by $Bu_3SnC_6F_{13}$ can plausibly be rationalised by the fact the electron-withdrawing C_2F_5 group attached to the δ-carbon in this compound effectively reduces the basicity of the fluorines attached to the γ- and δ-CF_2 centres.

CONCLUSIONS

In conclusion, the films produced from the perfluoroalkyltin compounds were encouraging, and showed that it was possible to grow a fluorine-doped tin oxide film from a single-source precursor. Overall, it appears that the best arrangement for a precursor in this class consists

of one containing a single fluorinated group. The length of the fluorinated chain seems to be important and for effective fluorine-doping a relatively small R_f group appears to be essential as the fluorine incorporation diminishes as R_f changed from C_4F_9 (**1**) to C_6F_{13} (**4**). For increased volatility and hence a significantly shorter run time, a vast improvement is achieved by the incorporation of small R groups (Et *vs* Bu), although film properties appear to be unaffected by the choice. Although organotin compounds containing small R groups are more expensive and have a higher toxicity than the corresponding butyltin compounds, the CVD properties are greatly enhanced.

Acknowledgements

We thank the Engineering and Physical Sciences Research Council for research studentships (B. F. J. and J. E. S.) and for support for the electron diffraction service (grant GR/R17768). We also thank Dr. V. Typke of the University of Ulm for the variable-array version of the ASYM40 program, Dr. S. L. Hinchley (Edinburgh) for assistance and Pilkington plc for financial support and help with the film analysis.

Supplementary Information

A complete set of calculated geometrical parameters for $Me_3SnC_4F_9$ (distances in pm) from the *ab initio* MO theory study (Table 2), interatomic distances (r_a/pm) and amplitudes of vibration (*u*/pm) for the restrained GED structure of $Me_3SnC_4F_9$ (Table 6), least-squares correlation matrix (x100) for $Me_3SnC_4F_9$ (Table 7), experimental and difference (experimental – theoretical) radial-distribution curves, *P(r)*/*r*, for $Me_3SnC_4F_9$ (Figure 4) and experimental and final weighted difference (experimental – theoretical) molecular-scattering intensities for $Me_3SnC_4F_9$ (Figure 5).

REFERENCES

1 Fillard JP, Manifacier JC. *Jpn. J. Appl. Phys.,* 1970; **9**:1012.

2 Tatsuyama C, Ichimura S. *Jpn. J. Appl. Phys.,* 1976; **15**:843.

3 Hass G, Heaney JB, Toft AR. *Appl. Opt.* 1979; **18**:1488.

4 Brinker DJ, Wang EY, Wadlin WH, Legge RN. *J. Electrochem. Soc.* 1981; **128**:1968.

5 Chopra KL, Major S, Pandya DK. *Thin Solid Films* 1983; **102**:1.

6 Das SK, Morris GC. *J. Appl. Phys.* 1993; **73**:782.

7 Ferrere S, Zaban A, Gregg BA. *J. Phys. B: At., Mol. Opt. Phys.* 1997; **101**:4490.

8 Ford WE, Wessls JM, Rodgers MAJ. *Journal of Physical Chemistry B* 1997; **101**:7435.

9 Laverty SJ, Feng H, Maguire P. *J. Electrochem. Soc.* 1997; **144**:2165.

10 Bélanger D, Dodelet JP, Lombos BA, Dickson JI. *J. Electrochem. Soc.* 1985; **132**:1398.

11 Upadhyay JP, Vishwakarma SR, Prasad HC. *Thin Solid Films* 1989; **169**:195.

12 Vishwakarma SR, Upadhyay JP, Prasad HC. *Thin Solid Films* 1989; **176**:99.

13 Haneko H, Miyake K. *J. Appl. Phys.* 1992; **53**:3629.

14 Lin Y-J, Wu C-J. *Surf. Coat. Technol.* 1996; **88**:239.

15 Proscia J, Gordon RG. *Thin Solid Films* 1992; **214**:175.

16 Ishida T, Tabata O, Park JW, Shin SH, Magara H, Tamura S, Mochizuki S, Mihara T. *Thin Solid Films* 1996; **281-282**:228.

17 Acosta DR, Zironi EP, Montoya E, Estrada W. *Thin Solid Films* 1996; **288**:1.

18 Chatelon JP, Terrier C, Bernstein E, Berjoan R, Roger JA. *Thin Solid Films* 1994; **247**:162.

19 Park S-S, Mackenzie JD. *Thin Solid Films* 1995; **258**:268.

20 Racheva TM, Critchlow GW. *Thin Solid Films* 1997; **292**:299.

21 Ray SC, Karanjai MK, DasGupta D. *Surf. Coat. Technol.* 1998; **102**:73.

22 Gamard A, Jousseaume B, Toupance T, Campet G. *Inorg. Chem.* 1999; **38**:4671.

23 Gamard A, Babot O, Jousseaume B, Rascle M-C, Toupance T, Campet G. *Chem. Mater.* 2000; **12**:3419.

24 Minami T, Nanto H, Takata S. *Japanese Journal of Applied Physics* 1988; **27**:L287.

25 Geoffroy C, Campet G, Menil F, Portier J, Salardenne J, Couturier G. *Active Passive Elec. Comput.* 1991; **14**:111.

26 Karlsson T, Roos A, Ribbing C-G. *Sol. Energy Mater.* 1985; **11**:469.

27 Yagi I, Ikeda E, Kuniya Y. *J. Mater. Res.* 1994; **9**:663.

28 Gordillo G, Moreno LC, de la Cruz W, Teheran P. *Thin Solid Films* 1994; **252**:61.

29 Laurent J-M, Smith A, Smith DS, Bonnet J-P, Clemente RR. *Thin Solid Films* 1997; **292**:145.

30 Shanthi S, Subramanian C, Ramasamy P. *Mater. Sci. Eng., B* 1999; **57**:127.

31 Karlsson B, Valkonen E, Karlsson T, Ribbing C-G. *Thin Solid Films* 1981; **86**:91.

32 Granqvist CG. *Thin Solid Films* 1990; **193**:730.

33 Nikodem RB. *J. Vac. Sci. Technol., A* 1992; **10**:1884.

34 Ghandhi SK, Siviy R, Borrego JM. *Appl. Phys. Lett.* 1979; **34**:833.

35 Borman CG, Gordon RG. *J. Electrochem. Soc.* 1989; **136**:3820.

36 Wan CF, McGrath RD, Keenan WF, Frank SN. *J. Electrochem. Soc.* 1989; **136**:1459.

37 Ghoshtagore RN. *J. Electrochem. Soc.* 1978; **125**:110.

38 Kojima M, Kato H, Imai A, Yoshida A. *J. Appl. Phys.* 1988; **64**:1902.

39 Yoon KH, Song JS. *Thin Solid Films* 1993; **224**:203.

40 Smith A, Laurent J-M, Smith DS, Bonnet J-P, Clemente RR. *Thin Solid Films* 1995; **266**:20.

41 Yusta FJ, Hitchman ML, Shamlian SH. *J. Mater. Chem.* 1997; **7**:1421.

42 Atagi LM, Hoffman DM, Liu J-R, Zheng Z, Chu W-K. *Chem. Mater.* 1994; **6**:360.

43 Tan C, Xia Y, Chen Y, Li S, Liu J, Liu X, Xu B. *J. Appl. Phys.* 1983; **73**:4266.

44 Ma HL, Zhang DH, Win SZ, Li SY, Chen YP. *Sol. Energy Mater.* 1996; **40**:371.

45 Yoon KH, Song JS. *Sol. Energy Mater.* 1993; **28**:317.

46 Saxena AK, Thangaraj R, Singh SP, Agnihotri OP. *Bull. Mater. Sci.* 1986; **8**:315.

47 Athey PR, Urban III FK, Holloway PH. *J. Vac. Sci. Technol., B* 1996; **14**:3436.

48 Clark HC, O'Brien RJ, Trotter J. *J. Chem. Soc. C,* 1964; 2332.

49 Tudela D, Gutiérrez-Puebla E, Monge A. *J. Chem. Soc., Dalton Trans.* 1992; 1069.

50 Boegeat D, Jousseaume B, Toupance T, Campet G, Fournès L. *Inorg. Chem.* 2000; **39**:3924.

51 Suh S, Hoffman DM, Atagi LM, Smith DS, Liu J-R, Chu W-K. *Chem. Mater.* 1997; **9**:730.

52 Suh S, Hoffman DM. *Inorg. Chem.* 1996; **35**:6164.

53 Maruyama T, Tabata K. *J. Appl. Phys.* 1990; **68**:4282.

54 Suh S, Zhang Z, Chu W-K, Hoffman DM. *Thin Solid Films* 1999; **345**:240.

55 Franc C, Jousseaume B, Linker M, Toupance T. *Chem. Mater.* 2000; **12**:3100.

56 Boutet S, Gamard A, Jousseaume B, Toupance T, Campet G, Cachet H. *Main Group Met. Chem.* 2002; **25**:59.

57 Cullen WR, Sams JR, Waldman MC. *Inorg. Chem.* 1970; **9**:1682.

58 Keasz HD, Phillips JR, Stone FGA. *J. Am. Chem. Soc.* 1960; **82**:6228.

59 Clark HC, Willis CJ. *J. Am. Chem. Soc.* 1960; **82**:1888.

60 Uno H, Shiraishi Y, Suzuki H. *Bull. Chem. Soc. Jpn.* 1989; **62**:2636.

61 Stone FGA, Treichel PM. *Chem. Ind. (London)* 1960; 837.

62 Eujen R, Jahn N, Thurmann U. *J. Organomet. Chem.* 1994; **465**:153.

63 Seyferth D, Richter F. *J. Organomet. Chem.* 1995; **499**:131.

64 Kawakami K, Kuivila HG. *J. Org. Chem.* 1969; **34**:1502.

65 Burdon J, Coe PL, Haslock IB, Powell RL. *J. Chem. Soc., Chem. Commun.* 1996; 49.

66 Krause LJ, Morrison JA. *J. Chem. Soc., Chem. Commun.* 1980; 671.

67 Kitazume T, Ishikawa N. *Chem. Lett.* 1981; 1337.

68 Molloy KC, Purcell TG, Quill K, Nowell I. *J. Organomet. Chem.* 1984; **267**:237.

69 Edwards DA, Harker RM, Mahon MF, Molloy KC. *J. Mater. Chem.* 1999; **9**:1771.

70 Kaelble EF (1967) Scherrer eqn. In Handbook of X-rays. New York, McGraw-Hill, Ch. 17

71 Bass M (1995) Handbook of Optics, 2nd Edition ed. New York, McGraw Hill Inc.

72 Frisch MJ, Trucks GW, Schlegel HB, Gill PMW, Johnson BG, Robb MA, Cheesman JR, Keith TA, Petersson GA, Montgomery JA, Raghavachari K, Al-Laham MA, Zakrzewski VG, Ortiz JV, Foresman JB, Cioslowski J, Stefanov BB, Nanayakkara A, Challacombe M, Peng CY, Ayala PY, Chen W, Wong MW, Andres JL, Replogle ES, Gomperts R, Martin RL, Fox DJ, Binkley JS, Defrees DJ, Baker J, Stewart JP, Head-

Gordon M, Gonzalez C, Pople JA (1995) Gaussian 94 (Revision C.2). In, Gaussian Inc., Pittsburgh, PA,

73 Dunning TH, Hay PJ (1976) Modern Theoretical Chemistry. In Ed. H. F. Schaefer I, ed. New York, Plenum, 1

74 Dunning TH. unpublished results;

75 Hay PJ, Wadt WR. *J. Chem. Phys.* 1985; **82**:270.

76 Wadt WR, Hay PJ. *J. Chem. Phys.* 1985; **82**:284.

77 Hay PJ, Wadt WR. *J. Chem. Phys.* 1985; **82**:299.

78 Hedberg L, Mills IM In

79 Hedberg L, Mills IM. *J. Mol. Spectrosc.* 1993; **160**:117.

80 Scott AP, Radom L. *J. Phys. Chem.* 1996; **100**:16502.

81 Huntley CM, Laurenson GS, Rankin DWH. *J. Chem. Soc., Dalton Trans.* 1980; 954.

82 Johnston BF, Rankin DWH, Turner AR ed@ed, Program for Analysis of Electron Diffraction Data. In, unpublished work

83 Ross AW, Fink M, Hilderbrand R (1992) International Tables for Crystallography. In Wilson AJC, ed. Dordrecht, Boston and London, Kluwer Academic Publishers, 245

84 Blake AJ, Brain PT, McNab H, Miller J, Morrison CA, Parsons S, Rankin DWH, Robertson HE, Smart BA. *J. Chem. Phys.* 1996; **100**:12280.

85 Mitzel NW, Smart BA, Blake AJ, Robertson HE, Rankin DWH. *J. Phys. Chem.* 1996; **100**:9339.

86 Mitchell TN. *J. Organomet. Chem.* 1973; **59**:189.

87 Nádvorník M, Holecek J, Handlir K, Lycka A. *J. Organomet. Chem.* 1984; **275**:43.

88 Parish RV, Platt RH. *J. Chem. Soc. A* 1969; 2145.

89 Agashe C, Marathe BR. *J. Phys. D: Appl. Phys.* 1993; **26**:2049.

90 Soubeyrand MJ, Halliwell AC. US Patent 5, 698, 262 (1997).

91 Fantini M, Torriani I. *Thin Solid Films* 1986; **138**:255.

92 Kwon CW, Campet G, Portier J, Poquet A, Fournès L, Labrugère C, Jousseaume B, Toupance T, H CJ, Subramanian MA. *Int. J. Inorg. Mat.* 2001; **3**:211.

93 Stanley JE, Molloy KC, Mahon MF, Rankin DWH, Robertson HE, Johnston BF. *submitted for publication*

Table 1. Known synthetic routes to fluoroalkyltin compounds

COMPOUND	Yield	Synthesis[a]	Comments	Ref.
Me_3SnCF_3	42	R_3SnSnR_3 + R_fI	Reaction involves Carius tube, difficult to separate complex product mixture.	58
$Me_3SnC_2F_5$	17			57
$Me_3SnCF(CF_3)_2$	42			57
$Me_2Sn(C_2F_5)_2$	34	Mg + R_fI; n R_fMgI + $R_{4-n}SnX_n$	Slow reaction, low yields.	61
$Bu_2Sn(C_2F_5)_2$	16			61
$Bu_3SnC_2F_5$	48			61
$Sn(C_3F_7)_4$	19	$^{i}PrMgI$ + R_fI; n R_fMgI + $R_{4-n}SnX_n$	Good method provided careful control of low temperature is maintained.	63
$MeSn(C_3F_7)_3$	11			63
$Me_2Sn(C_3F_7)_2$	82			63
$Bu_3SnC_4F_9$	28	MeLi + R_fI; n R_fLi + $R_{4-n}SnX_n$	Method unreliable, complex product mixture.	60

Table 2. Calculated geometrical parameters (distances/pm, angles/deg) for the three lowest energy conformers of $Me_3SnC_4F_9$ calculated at the MP2/LanL2DZ (Sn) – D95 level.

(a) bond lengths

	Conformer 1	Conformer 2	Conformer 3
Sn(1)-C(6)	213.3	213.2	213.2
Sn(1)-C(7)	213.3	213.1	213.3
Sn(1)-C(8)	213.3	213.3	213.2
Sn(1)-C(2)	221.6	221.7	221.7
C(2)-C(3)	152.4	152.2	152.7
C(3)-C(4)	153.9	153.9	153.5
C(4)-C(5)	153.7	153.4	153.6
C(2)-F(9)	138.9	138.5	138.5
C(2)-F(10)	138.1	138.6	138.9
C(3)-F(11)	137.0	137.2	136.3
C(3)-F(12)	136.6	136.3	136.5
C(4)-F(13)	135.6	135.6	135.7
C(4)-F(14)	135.9	136.2	136.9
C(5)-F(15)	134.2	134.4	134.4
C(5)-F(16)	134.4	134.1	133.9
C(5)-F(17)	134.0	134.2	134.2

(b) inter-bond angles

	Conformer 1	Conformer 2	Conformer 3
C(2)-Sn(1)-C(6)	103.2	103.7	101.8
C(2)-Sn(1)-C(7)	105.8	105.7	107.3
C(2)-Sn(1)-C(8)	106.9	107.5	107.6
C(7)-Sn(1)-C(8)	113.6	112.9	113.9
Sn(1)-C(2)-C(3)	115.3	115.3	121.7
C(2)-C(3)-C(4)	116.3	119.2	114.7
C(3)-C(4)-C(5)	114.5	117.2	115.4
F(9)-C(2)-F(10)	107.1	107.1	104.2
F(11)-C(3)-F(12)	107.9	108.1	108.6
F(13)-C(4)-F(14)	109.3	108.8	108.4
Sn(1)-C(2)-F(9)	109.5	109.9	109.7
Sn(1)-C(2)-F(10)	110.7	110.5	107.3
C(2)-C(3)-F(11)	107.9	107.6	110.2
C(2)-C(3)-F(12)	108.1	108.0	108.0

C(3)-C(4)-F(13)	108.7	109.0	110.2
C(3)-C(4)-F(14)	109.5	106.9	107.7
C(4)-C(5)-F(15)	109.2	108.8	108.9
C(4)-C(5)-F(16)	110.1	110.6	110.5
C(4)-C(5)-F(17)	110.8	110.5	110.4

(c) torsion angles

	Conformer 1	Conformer 2	Conformer 3
C(3)-C(2)-Sn(1)-C(6)	166.2	157.3	164.6
Sn(1)-C(2)-C(3)-C(4)	164.8	167.1	55.7
C(2)-C(3)-C(4)-C(5)	161.6	53.5	168.4
C(3)-C(4)-C(5)-F(15)	169.1	169.5	169.3
C(2)-Sn(1)-C(6)-H(21)	179.8	178.5	178.6
H(20)-C(7)-Sn(1)-C(6)	31.3	62.8	50.4
H(26)-C(8)-Sn(1)-C(6)	63.4	173.2	53.6

Table 3. Nozzle-to-plate distances (mm), weighting functions (nm^{-1}), correlation parameters, scale factors and electron wavelengths (pm) used in the electron-diffraction study of $Me_3SnC_4F_9$.

Nozzle-to-plate distance[a]	95.57	252.33
Δs	40	20
s_{min}	112	30
s_{w1}	132	50
s_{w2}	212	94
s_{max}	248	110
Correlation parameter	0.0185	-0.3792
Scale factor[b]	0.343(16)	0.895(10)
Electron wavelength	6.016	6.016

[a] Determined by reference to the scattering pattern of benzene vapour.

[b] Values in parentheses are the estimated standard deviations.

Table 4. Refined and calculated geometric parameters for $Me_3SnC_4F_9$ (distances in pm, angles in °) from the GED study.[a, b]

No.	Parameter	GED (r_a)	MP2/Lan2DZ (Sn) - D95	Restraint
p_1	C-H av.	109.5(7)	109.3	109.8(13)
p_2	Sn-C av.	214.7(5)	215.4	215.6(23)
p_3	[Sn(1)-C(2)] – [Sn(1)-C(6/7/8)]	9.0(5)	8.4	9.0(5)
p_4	C-C av.	155.0(3)	153.2	154.8(4)
p_5	C-F av.	135.9(1)	136.1	136.0(32)
p_6 [c]	Δ C(2)-F(9/10)	3.3(2)	3.2	3.3(2)
p_7 [c]	Δ C(3)-F(11/12)	1.9(1)	1.7	1.9(1)
p_8 [c]	Δ C(4)-F(13/14)	1.3(1)	1.8	1.3(1)
p_9	C(4)-C(5)-F(15/16/17) av.	109.7(4)	109.9	110.2(5)
p_{10}	F-C-F	107.7(4)	107.7	107.7(5)
p_{11}	C(3)-C(4)-C(5) in conf. 2	117.0(8)	117.2	117.2(10)
p_{12}	C(2)-C(3)-C(4) in conf. 2	120.0(5)	119.2	120.2(5)
p_{13}	Sn(1)-C(2)-C(3) in conf. 2	116.8(9)	115.3	115.7(11)
p_{14}	C(2)-Sn(1)-C(6)	102.9(5)	102.9	102.8(5)
p_{15}	C(7)-Sn(1)-C(8)	107.0(9)	113.5	106.5(10)
p_{16}	C(6)-Sn(1)-C(7/8) av.	113.4(5)	112.9	113.4(5)
p_{17}	Sn-C-H av.	110.7(5)	110.8	110.8(5)
p_{18}	C(3)-C(4)-C(5) in conf. 1	114.4(5)	114.5	114.5(5)
p_{19}	C(2)-C(3)-C(4) in conf. 1	116.7(5)	116.3	117.0(5)
p_{20}	Sn(1)-C(2)-C(3) in conf. 1	117.6(7)	115.3	115.5(13)
p_{21}	C(3)-C(4)-C(5) in conf. 3	115.9(5)	115.4	115.9(5)
p_{22}	C(2)-C(3)-C(4) in conf. 3	114.2(10)	114.7	114.1(10)
p_{23}	Sn(1)-C(2)-C(3) in conf. 3	122.0(14)	121.7	122.0(15)
p_{24} [c]	*Anti* twist	164.6(17)	164.3	
p_{25} [c]	*Gauche* twist	12.1(23)	54.6	
p_{26}	CF_3 twist	184.0(19)	169.3	169.2(5)
p_{27}	Weight conf. 2	0.65	0.49	
p_{28}	Weight conf. 1	0.33	0.38	

[a] Figures in parentheses are the estimated standard deviations of the last digits.

[b] Unless stated, parameter definitions apply to all three conformers.

[c] See text for a full definition.

Table 5. Properties of deposited F:SnO_2 films

PRECURSOR	(**1**)	(**2**)	(**3**)	(**4**)	(**5**)	**Standard** [a]
Thickness (Å)	3795	3675	6165	2000	4330	3000
Haze (%)	0.64	0.54	4.10	0.50	1.05	< 0.40
Emissivity	0.220	0.328	0.139	0.655	0.132	< 0.150
Sheet Resistance (Ω/□) [b]	22	58	9	215	11	15
Resistivity ($\times 10^{-3}$ Ω cm)	0.85	2.13	0.58	5.10	0.46	0.50
Fluorine Content (atom%)	1.48	2.02	0.79	< 0.05	1.20	2.00

[a] Typical measurements for a commercial fluorine-doped tin oxide film derived from separate tin and fluorine sources.[90]

[b] □ = 25 mm^2

Figure Captions

Figure 1. *Ab initio* structures and numbering schemes of the conformers of $Me_3SnC_4F_9$. (a) lowest energy conformer (1), (b) conformer (2) 0.8 kJ mol^{-1} above the minimum, (c) conformer (3) 4.5 kJ mol^{-1} higher in energy than the minimum, (d) conformer (4) 16.6 kJ mol^{-1} above the minimum.

Figure 2. X-Ray Diffraction Pattern for the F:SnO_2 film grown from $Bu_3SnC_4F_9$ (**1**)

Figure 3. Scanning Electron Micrographs of the F:SnO_2 film grown from $Bu_3SnC_4F_9$ (**1**)

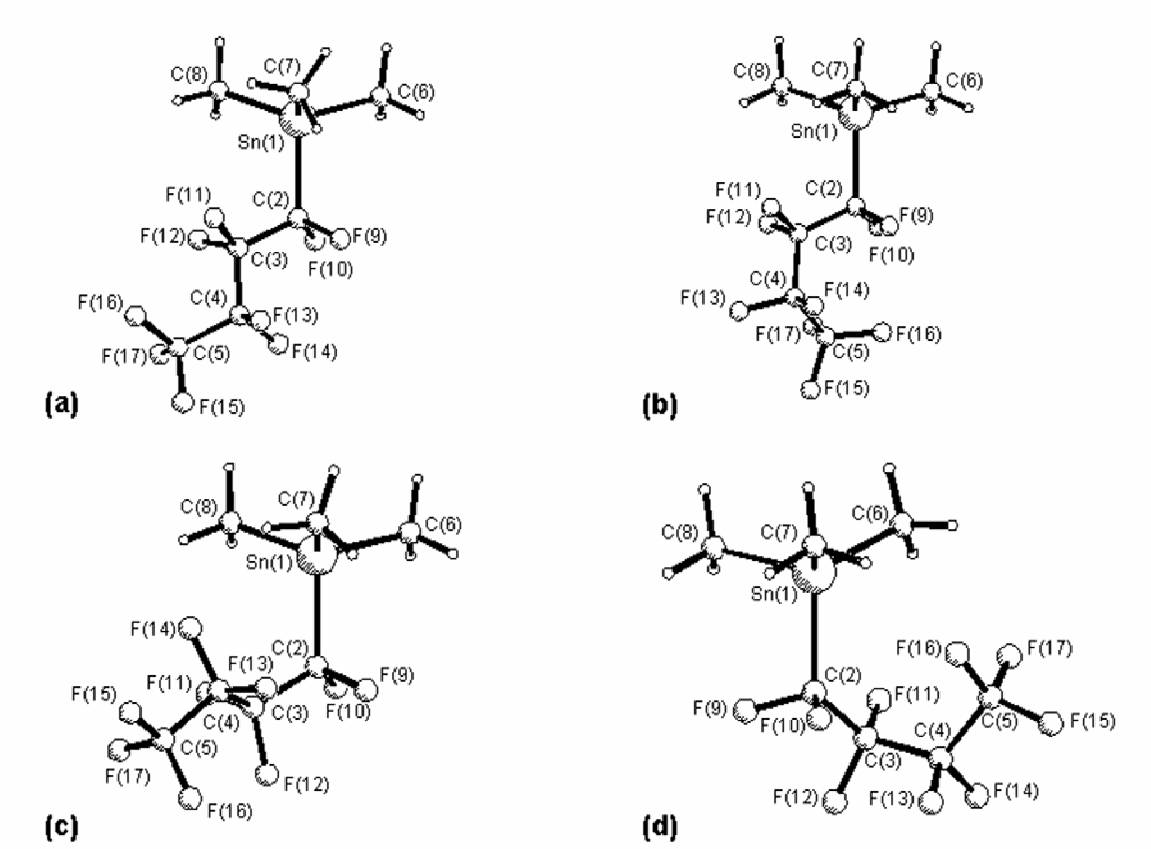
C(8)
C(7)
C(6)
Sn(1)
F(11)
C(2)
F(12)
F(9)
C(3)
F(10)
F(16)
C(4)
F(13)
F(17)
C(5)
F(14)
F(15)
(a)
C(8)
C(7)
C(6)
Sn(1)
F(11)
C(2)
F(12)
F(9)
C(3)
F(10)
C(4)
F(13)
F(14)
F(17)
F(16)
C(5)
F(15)
(b)
C(8)
C(7)
C(6)
Sn(1)
F(14)
C(2)
F(13)
F(9)
F(11)
F(15)
C(4)
C(3)
F(10)
C(5)
F(17)
F(12)
F(16)
(c)
C(8)
C(7)
C(6)
Sn(1)
F(16)
F(17)
C(2)
F(9)
F(11)
C(5)
F(15)
F(10)
C(4)
C(3)
F(12)
F(13)
F(14)
(d)

Figure 1

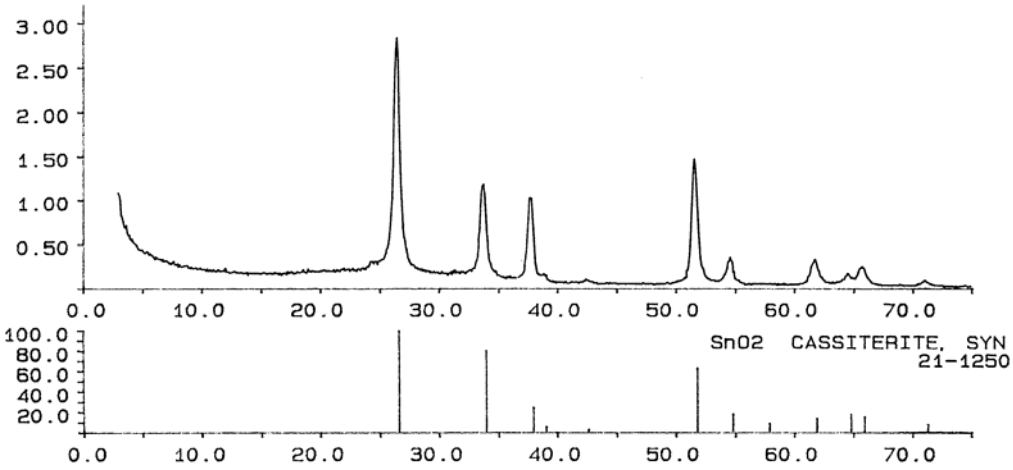
3.00
2.50
2.00
1.50
1.00
0.50
0.0
10.0
20.0
30.0
40.0
50.0
60.0
70.0
100.0
80.0
60.0
40.0
20.0
SnO2 CASSITERITE, SYN
21-1250

Figure 2